2019 International Conference on Robotics and Automation (ICRA)
Palais des congres de Montreal, Montreal, Canada, May 20-24, 2019

Robust attitude estimation using an adaptive unscented Kalman filter

Antonio C. B. Chiella, Bruno O. S. Teixeira, and Guilherme A. S. Pereira

Abstract— **This paper presents the robust Adaptive unscented Kalman filter (RAUKF) for attitude estimation. Since the proposed algorithm represents attitude as a unit quaternion, all basic tools used, including the standard UKF, are adapted to the unit quaternion algebra. Additionally, the algorithm adopts an outlier detector algorithm to identify abrupt changes in the UKF innovation and an adaptive strategy based on covariance matching to tune the measurement covariance matrix online. Adaptation and outlier detection make the proposed algorithm robust to fast and slow perturbations such as magnetic field interference and linear accelerations. Experimental results with a manipulator robot suggest that our method overcomes other algorithms found in the literature.**

I. Introduction

Attitude estimation is a crucial task for a variety of applications, such as human motion tracking [1], augmented reality [2], satellite control [3] and navigation and control of aerial [4], and sub-aquatic vehicles [5]. In these applications, orientation information is usually provided by an attitude and heading reference system (AHRS).

With the raising of small flying vehicles, also known as drones, small and inexpensive AHRS have populated the market. For such systems, it is common to estimate the orientation by combining information from a magnetic, rate and gravity (MARG) sensor, also known as inertial measurement unit (IMU), usually composed of micromechanical (MEMS) three-axis gyroscope and accelerometer and a three-axis magnetometer [6]. The standard approach for attitude estimation is to compute the three components of inertial orientation by integrating the gyroscope measurements, and use the gravity projection and heading angle estimated by the accelerometers and magnetometers to correct the angles estimated with the gyro. Although theoretically simple, naive implementations of this approach may not be precise because magnetometer measurements are easily influenced by ferrous material in the vicinity, and accelerometers measure not only the gravitational direction but also linear acceleration. In these cases, it is difficult to dissociate magnetic field perturbation and linear acceleration from both the magnetic field of the earth and gravity to compute the attitude accurately, which can lead to poor estimates [7]. To present an alternative solution to these problems is one of the main objectives of this paper.

The most intuitive way of describing attitude is by using Euler angles, where the attitude is broken into three successive rotations. However, Euler angles exhibit singularity in the kinematic description, which is known as gimbal lock. In contrast, unit quaternion and direct cosine representations avoid such singularities. Unit quaternion is preferred due to its minimal representation and computational efficiency [8]. However, the unit quaternion representation does not pertain to the Euclidean space, which means that weighted sum operations, common to most sensor fusion methodologies, may violate the unit norm constraint of the quaternion. This paper proposes a solution to this problem in situations where the uncertainty of the measurements may change over time.

The main contribution of this paper is the proposition of the robust adaptive unscented Kalman filter (RAUKF) algorithm for attitude estimation. This algorithm is robust to fast and slow perturbations on both accelerometers and magnetometers and, to the best of authors' knowledge, is the first one with such characteristics that precisely and consistently represent the attitude using quaternions. The proposed algorithm is tested with real experimental data collected from a MARG sensor. The performance of the proposed algorithm is confronted against the non-adaptive UKF, the open source algorithm based on complementary filter proposed in [9] and the commercial algorithm embedded in the MARG device used in our experiments, which was executed using a manipulator robot for validation purposes.

II. Literature Review

There are many approaches to estimate attitude using the quaternion representation. Among the stochastic approaches, techniques based on the Kalman filter (KF) are the most common [10]. The issue with KF is that it pertains to the Euclidean systematization, thus the unit norm constraints are not ensured in standard approaches. To overcome this limitation, an indirect form of the KF, called multiplicative extended Kalman filter (MEKF) [11], was proposed. This approach is valid only for small estimation errors. For large errors, algorithms based on the unscented Kalman filter (UKF) as the unscented quaternion estimator (USQUE) [12] may yield better results. Since unit quaternions are constrained to the nonlinear Riemannian manifold, using its *logarithm* and *exponential* maps, as in [8], [13], can better handle its properties. A more general formulation of UKF for unit quaternion can be found in [14]. However, these algorithms do not explore the time-varying measurement uncertainty. For example, if disturbance affects the measurement of the magnetic field, the filter estimate will be severely damaged.

This work was partially supported by FAPEMIG/Brazil, grant TEC-APQ-00850-15, CNPq/Brazil, grant 465755/2014-3 (INCT) and CAPES/Brazil grant 88887.136349/2017-00. A. Chiella holds a scholarship from CAPES/Brazil. B. Teixeira and G. Pereira hold research fellowships from CNPq/Brazil.

A.Chiella and B.Teixeira are with the Graduate Program in Electrical Engineering, School of Engineering, Universidade Federal de Minas Gerais, Brazil acbchiella@ufmg.br, brunoot@ufmg.br

G.Pereira is with the Mechanical and Aerospace Engineering Department, West Virginia University, USA. During the realization of this work he was with School of Engineering, Universidade Federal de Minas Gerais, Brazil. guilherme.pereira@mail.wvu.edu

The classical way of handling the temporal variation of uncertainty is through adaptive filters, in which the statistical parameters that characterize the uncertainty are jointly estimated with the system states. In this context, approaches based on the techniques referred to as covariance matching (CM) [15], interacting multiple models (IMM) [16] and covariance scaling (CS) [17], were investigated. Among these methods, the covariance matching approaches yield improved results in the estimation of the covariance matrix for Gaussian distribution, if compared to the CS approach, and also a greater simplicity compared to approaches based on multiple models. However, in the presence of outliers, its performance can be damaged. In this context, median-based approaches can be combined to mitigate the outlier influence [18], [19]. It is important to point out that, like the KF, these adaptive approaches also belong to Euclidean systematization, thus requiring modifications to be used with unitary quaternions.

In [20], the authors present an adaptive UKF for attitude estimation. The adaptive part of the algorithm is based on a covariance scaling approach which adapts the covariance matrix if a fault is detected by using a chi-square test. The main shortcoming of this approach is that, if the chi-square test fails, e.g. for a slow varying fault, the algorithm does not modify the covariance matrix. In addition, the attitude is parameterized by Euler angles, being vulnerable to gimbal-lock. Based on the algorithms shown in [12] and [20], an adaptive UKF for attitude represented in quaternions is presented in [21]. In [22], a inflated covariance method based on multiplicative EKF (MEKF) is proposed to compensate the undesired effects of magnetic distortion and body acceleration. In spite of demonstrated good performance in numerically simulated cases, this algorithm suffers the same limitation of MEKF.

In contrast to the KF approaches, which adopt a probabilistic determination of the modeled state, complementary filters (CF) are based on frequency analysis, being simplistic and usually computationally more efficient. In [23], the authors proposed an explicit complementary filter (ECF) for orientation estimation. Such a filter uses a proportional-integral (PI) controller to estimate the bias of the gyro. In [24], the authors present a computationally efficient gradient descent algorithm given measurements from a MARG sensor. The proposed algorithm has low computational cost and is able to reduce the effect of the magnetic disturbance. The problem of this algorithm is that the orientation estimated using accelerometers suffer the influence of magnetic disturbances due to the coupling in the gradient descent algorithm used. In [25], quaternion measurement is computed as the composition of two algebraic quaternions, mitigating the influence of magnetic distortion. Adaptive gains are used to reduce the estimation error during high dynamic motion.

In this scenario, we propose an adaptive algorithm based on UKF for attitude estimation using quaternion representation, see Section V-D. The unit norm constraint is ensured by the use of the rotation vector parameterization, as in [8], [14]. In the proposed algorithm, an indirect measurement of the unit quaternion is used to correct the gyro estimates. The unit quaternion is computed from MARG sensor measurements as in [10]. The adaptive part of the algorithm is based on covariance matching [15]. To minimize the effect of measurement outliers, the adaptive filter is combined with a Hampel identifier [26], which compares the median deviation and the median absolute deviation (MAD) to identify an outlier.

III. Quaternion Operations

Unit quaternions form a 4-dimensional algebra over the real numbers and can be used to parametrize the rotation group SO(3). The set of unit quaternions, denoted by $\mathbb{H}_1$, form the group $\mathcal{S}^3$ under multiplication operation [14].

A. Algebra of Unit Quaternions

The unit quaternion can be represented as $e = (v,\, n) \in \mathbb{H}_1$, in which $\|e\| = 1$. Here $v \in \mathbb{R}$ is the real part and $n \in \mathbb{R}^3$ is the imaginary part. Given a rotation θ and the unit vector w, the corresponding unit quaternion is $e = \left(\cos\left(\frac{\theta}{2}\right),\, \sin\left(\frac{\theta}{2}\right) w\right)$. The inversion unit quaternion operation is equals to its conjugate, given by $e^{-1} = e^* = (v,\, -n)$. The product $\otimes$ between quaternions is defined as $e_a \otimes e_b \triangleq \left(v_a v_b - n_a^T n_b,\, v_a n_b + v_b n_a + n_a \times n_b\right)$, in which $\times$ denotes the cross product [27]. A vector $v \in \mathbb{R}^3$ can be rotated by a unit quaternion e, which is given by $(0,\, u) = e\,(0,\, v)\,e^*$, where $u \in \mathbb{R}^3$ is the rotated vector [8].

B. Euclidean Tangent Space and Rotation Vector Parametrization

The group $\mathcal{S}^3$ is a Riemannian manifold, whose elements can be represented in a 3-dimensional Euclidean *tangent space* $\mathrm{T}_e\mathcal{S}^3$. Many operations are defined in the Euclidean tangent space, such as the empirical mean and covariance. Furthermore, there are direct and inverse mappings between the manifold and its *tangent space*, $\mathcal{S}^3 \longleftrightarrow \mathrm{T}_e\mathcal{S}^3$, with *exponential* and *logarithm* functions, respectively.

Let $e = (v,\, n)$ be a unit quaternion and $r = \frac{\theta}{2} w$ be a rotation vector representing a rotation θ about the unit axis w. The unit quaternion to *rotation vector* mapping, called *logarithm* mapping, is given by [14]:

$$r = \begin{cases} 2\arccos(v)\,\frac{n}{\|n\|},\ \text{if } \|n\| \neq 0\,, \\ [0]_{3\times 1}\,,\ \text{if } \|n\| = 0\,. \end{cases} \tag{1}$$

The inverse mapping, called *exponential* mapping, is [14]:

$$e = \begin{cases} \left(\cos\left(\frac{\|r\|}{2}\right),\, \sin\left(\frac{\|r\|}{2}\right)\frac{r}{\|r\|}\right),\ \text{if } \|r\| \neq 0\,, \\ (1,\, [0]_{3\times 1})\,,\ \text{if } \|r\| = 0\,. \end{cases} \tag{2}$$

For brevity, *logarithm* (1) and *exponential* (2) mappings are written as $e = \mathrm{R2Q}(r)$ and $r = \mathrm{Q2R}(e)$, respectively.

C. Sum, Subtraction, and Weighted Mean Operations

We define now the operations of sum, subtraction, and weighted mean for unit quaternion states.

The difference between e_a and $e_b \in \mathbb{H}_1$ is defined as

$$e_a \ominus e_b \triangleq \mathrm{Q2R}\left(e_a \otimes e_b^*\right)\,. \tag{3}$$

The sum of a unit quaternion $e_a \in \mathbb{H}_1$ and a rotation vector $r \in \mathbb{R}^3$, is defined as

$$e_a \oplus r \triangleq \mathrm{R2Q}\,(r) \otimes e_a\,. \tag{4}$$

Lastly, the weighted mean operation for a set of unit quaternions $E = \{e_i\}$, $i \triangleq 1 \ldots n_w$, is defined as

$$\hat{e} \triangleq \mathrm{WM}\,(E, W)\,, \tag{5}$$

where $W = \{w_i\}$ is a set of corresponding weights. In this work, the gradient descent algorithm presented in [8] is used.

D. Quaternion Unscented Transform

The *unscented* transform (UT) is the main core of UKF. The UT approximates the mean $\hat{y} \in \mathbb{R}^m$ and its covariance $P^{yy} \in \mathbb{R}^{m\times m}$ of a random variable y obtained from the nonlinear transformation $y = h(x_1, x_2, c)$, where $x_1 \in \mathbb{R}^{n_1}$ and $x_2 \in \mathbb{R}^{n_2}$ are random variables with mean $\hat{x}_1$ e $\hat{x}_2$ and covariance matrices $P^{x_1x_1} \in \mathbb{R}^{(n_1-1)\times(n_1-1)}$ and $P^{x_2x_2} \in \mathbb{R}^{n_2\times n_2}$, respectively, and c a known deterministic variable. In addition, the random variable x_1 is composed by a unit quaternion part $x_{1,\mathrm{H}}$ and a unconstrained Euclidean part $x_{1,\mathrm{E}}$; thus $x_1 \triangleq \left[x_{1,\mathrm{H}}^T\, x_{1,\mathrm{E}}^T\right]^T$.

Now, we define the augmented state vector $\breve{x} \in \mathbb{R}^{\breve{n}}$ as

$$\breve{x} \triangleq \left[\, x_1^T\ x_2^T \,\right]^T, \tag{6}$$

where $\breve{n} = n_1 + n_2$, as well as the augmented covariance matrix $P^{\breve{x}\breve{x}} \in \mathbb{R}^{(\breve{n}-1)\times(\breve{n}-1)}$

$$P^{\breve{x}\breve{x}} = \begin{bmatrix} P^{x_1x_1} & [0]_{(n_1-1)\times n_2} \\ [0]_{n_2\times(n_1-1)} & P^{x_2x_2} \end{bmatrix}. \tag{7}$$

The UT is based on a set of deterministically chosen samples known as sigma points (SP). The sigma points $\mathcal{X}_j \in \mathbb{R}^{\breve{n}-1}$ and the associated weights w_j, $j = 1, \ldots, 2(\breve{n}-1)$ can be chosen as

$$\mathcal{X} = \hat{\breve{x}}\,[1]_{1\times 2(\breve{n}-1)} \oplus \sqrt{\breve{n}-1}\left[\left(P^{\breve{x}\breve{x}}\right)^{\frac{1}{2}}\ -\left(P^{\breve{x}\breve{x}}\right)^{\frac{1}{2}}\right], \tag{8}$$

$$w_j = \frac{1}{2(\breve{n}-1)}, \tag{9}$$

where $\mathcal{X}_j$ is the jth column of matrix $\mathcal{X} \in \mathbb{R}^{(\breve{n}-1)\times 2(\breve{n}-1)}$, $(\cdot)^{\frac{1}{2}}$ is the Cholesky square root operation, and $[1]_{1\times 2(\breve{n}-1)} \in \mathbb{R}^{1\times 2(\breve{n}-1)}$ is a row vector with elements equal to one. Notice that, the columns of the covariance matrix $P^{\breve{x}\breve{x}}$ can be seen as a perturbation variable, where the unit quaternion part is parameterized as a *rotation vector*, which means that the covariance matrix is defined in the *tangent space*, hence the $\breve{n}-1$ dimension. The SP (8) can be partitioned as

$$\begin{bmatrix} \mathcal{X}^{x_1} \\ \mathcal{X}^{x_2} \end{bmatrix} \triangleq \mathcal{X}, \tag{10}$$

where $\mathcal{X}^{x_1} \in \mathbb{R}^{(n_1-1)\times 2(\breve{n}-1)}$ and $\mathcal{X}^{x_2} \in \mathbb{R}^{n_2\times 2(\breve{n}-1)}$.

Then each sigma point $\mathcal{X}_j$ is propagated through h:

$$\mathcal{Y}_j = h\left(\mathcal{X}_j^{x_1}, \mathcal{X}_j^{x_2}, c\right), \tag{11}$$

where $\mathcal{Y}_j = \left[\mathcal{Y}_{j,\mathrm{H}}^T\, \mathcal{Y}_{j,\mathrm{E}}^T\right]^T \in \mathbb{R}^{n_y}$ is the jth column of the matrix $\mathcal{Y} \in \mathbb{R}^{n_y\times 2(\breve{n}-1)}$.

From (11), we obtain $\hat{y}$, P^{yy} and P^{x_1y} as

$$\hat{y} = \mathrm{WM}\,(\mathcal{Y}, w)\,, \tag{12}$$

$$P^{yy} = \sum_{j=1}^{2(\breve{n}-1)} w_j\,(\mathcal{Y}_j \ominus \hat{y})\,(\mathcal{Y}_j \ominus \hat{y})^T\,, \tag{13}$$

$$P^{x_1y} = \sum_{j=1}^{2(\breve{n}-1)} w_j\left(\mathcal{X}_j^{x_1} \ominus x_1\right)(\mathcal{Y}_j \ominus \hat{y})^T\,. \tag{14}$$

At this point it is important to mention that equations (8) and (12)-(14) differ from the one in the standard UT transform because they consider the quaternion operations previously defined in this section [28].

From now on, for notation simplicity, we define the quaternion unscented transformation as the function UT$(\cdot)$ comprising the set of equations (8)-(14) as:

$$\{\hat{y}, P^{yy}, P^{xy}\} = \mathrm{UT}\left(\hat{\breve{x}}, P^{\breve{x}\breve{x}}, c, h\right). \tag{15}$$

where $\hat{\breve{x}}$ and $P^{\breve{x}\breve{x}}$ are given by (6) and (7), respectively.

IV. Mathematic Modeling

This section describes the discrete time dynamic model used by the filtering algorithm presented in this paper.

A. Kinematic Model of Attitude

Assuming that angular rates $\omega_k \in \mathbb{R}^3$, measured by a 3-axis gyros form the input vector u_k of the dynamic system, the discrete-time attitude model is given by [12]

$$\mathrm{vec}\,(e_k) = A_{k-1}\mathrm{vec}\,(e_{k-1})\,, \tag{16}$$

where $\mathrm{vec}\,(\cdot) : \mathbb{H}_1 \to \mathbb{R}^4$ is an operator that takes the four coefficients of the unit quaternion and stacks them in a 4-vector, k denotes the discrete time, and

$$A_{k-1} \triangleq \mathrm{c}\left(\frac{T}{2}||\omega||\right)\mathrm{I}_{4\times 4} + \frac{T}{2}\mathrm{s}\left(\frac{T}{2}||\omega||\right)\Omega(\omega)\,,$$

$$\Omega(\omega) \triangleq \begin{bmatrix} 0 & -\omega_x & -\omega_y & -\omega_z \\ \omega_x & 0 & \omega_z & -\omega_y \\ \omega_y & -\omega_z & 0 & \omega_x \\ \omega_z & \omega_y & -\omega_x & 0 \end{bmatrix}.$$

We assume that $u_k = \omega_k \in \mathbb{R}^3$ is corrupted by random noise and bias terms, modeled as $u_{\mathrm{m},k} = u_k + \beta_k + q_{\mathrm{u},k}$, in which "m" denotes a measured variable, $u_{\mathrm{m},k} = [\omega_{x_\mathrm{m}}\ \omega_{y_\mathrm{m}}\ \omega_{z_\mathrm{m}}]^T \in \mathbb{R}^3$ are angular rates measured by a 3-axis gyros, $\beta_k = [\beta_{\omega_x}\ \beta_{\omega_y}\ \beta_{\omega_z}]^T \in \mathbb{R}^3$ are bias terms, and $q_{\mathrm{u},k} \sim \mathcal{N}\left([0]_{3\times 1},\ Q_\mathrm{u}\right) \in \mathbb{R}^3$ is the input random noise. To directly use the measured inputs in (16), bias terms and random noise are estimated and subtracted from the measurement. Then, $u_k = u_{\mathrm{m},k} - \beta_k - q_{\mathrm{u},k}$.

Bias terms β_k are modeled as a random walk process,

$$\beta_k = \beta_{k-1} + q_{\beta,k-1}, \tag{17}$$

where $q_\beta \sim \mathcal{N}\left([0]_{3\times 1},\ Q_\beta\right) \in \mathbb{R}^3$ and are jointly estimated with the other system states, yielding a *joint state vector* $x_k \triangleq \left[\mathrm{vec}\,(e_k)\quad \beta_k^T\right]^T \in \mathbb{R}^7$.

Equations (16) and (17) compose the *process model*, which can be compactly presented as

$$x_k = f\left(x_{k-1},\, q_{k-1},\, u_{k-1},\, k-1\right), \tag{18}$$

where f denotes a nonlinear function of previous state x_{k-1}, with input u_{k-1}, and process noise $q_{k-1} \triangleq \begin{bmatrix} q_{\mathrm{u},k-1}^T & q_{\beta,k-1}^T \end{bmatrix}^T$.

B. Observation Model

The observation model relates the components of state vector x_k with the output measurement vector $y_k \in \mathbb{H}_1$, defined as $y_k \triangleq e_{\mathrm{m}}$. Measurements are corrupted by random errors and modeled as $e_{\mathrm{m}} = e_k \oplus r_k$, where $r_k \sim \mathcal{N}\left([0]_{3\times 1}, R_k\right) \in \mathbb{R}^3$ is the measurement noise parameterized as a *rotation vector*. Therefore, the *observation model* may be written as

$$y_k = h\left(x_k,\, r_k,\, k\right). \tag{19}$$

In this paper, the measured acceleration $a_{\mathrm{m},k} = \left[a_{\mathrm{x}}\ a_{\mathrm{y}}\ a_{\mathrm{z}}\right]^T \in \mathbb{R}^3$ and magnetic field $b_{\mathrm{m},k} = \left[b_{\mathrm{x}}\ b_{\mathrm{y}}\ b_{\mathrm{z}}\right]^T \in \mathbb{R}^3$ are used to compute the unit quaternion $e_{\mathrm{m}} \in \mathbb{H}_1$. Assuming normalized measurements such that $\|a_{\mathrm{m},k}\| = 1$ and $\|b_{\mathrm{m},k}\| = 1$, the unit quaternion representing the body attitude can be computed as [25], [10]:

$$e_{\mathrm{m}}^* = e_{\mathrm{acc}} \otimes e_{\mathrm{mag}}\,, \tag{20}$$

$$e_{\mathrm{acc}} = \begin{cases} \left(\lambda_1, \left[-\frac{a_{\mathrm{y}}}{2\lambda_1}\ \ \frac{a_{\mathrm{x}}}{2\lambda_1}\ \ 0\right]^T\right), & a_{\mathrm{z}} \geq 0 \\ \left(-\frac{a_{\mathrm{y}}}{2\lambda_2}, \left[\lambda_2\ 0\ \frac{a_{\mathrm{x}}}{2\lambda_2}\right]^T\right), & a_{\mathrm{z}} < 0, \end{cases} \tag{21}$$

$$e_{\mathrm{mag}} = \begin{cases} \left(\frac{\lambda_3}{\sqrt{2\Gamma}}, \left[0\ 0\ \frac{\lambda_3}{\sqrt{2\Gamma}}\right]^T\right), & l_{\mathrm{x}} \geq 0 \\ \left(\frac{l_{\mathrm{y}}}{\sqrt{2}\lambda_4}, \left[0\ 0\ \frac{\lambda_4}{\sqrt{2\Gamma}}\right]^T\right), & l_{\mathrm{x}} < 0, \end{cases} \tag{22}$$

where $\lambda_1 = \sqrt{(a_z+1)/2}$, $\lambda_2 = \sqrt{(1-a_z)/2}$, $\Gamma = l_{\mathrm{x}}^2 + l_{\mathrm{y}}^2$, $\lambda_3 = \sqrt{\Gamma + l_{\mathrm{x}}\sqrt{\Gamma}}$, $\lambda_4 = \sqrt{\Gamma - l_{\mathrm{x}}\sqrt{\Gamma}}$ and $l_{\mathrm{m},k} = \left[l_{\mathrm{x}}\ l_{\mathrm{y}}\ l_{\mathrm{z}}\right]^T$ such that$(0, l_{\mathrm{m},k}) = e_{acc}^*\left(0, b_{\mathrm{m},k}\right) e_{acc}$.

Because these equations are nonlinear, the unscented transform, given in (15), is used to propagate the measured acceleration $a_{\mathrm{m},k}$ and magnetic field $b_{\mathrm{m},k}$ errors through equations (20)–(22). These errors are modeled as zero mean random errors. In so doing, we obtain e_{m} used in (19).

V. State Estimators

We assume that the dynamic system is modeled by the nonlinear equations (18) and (19) in which, $\forall k \geq 1$, the known data are the measured output y_k and input u_{k-1}. It is also assumed that process noise $q_{k-1} \in \mathbb{R}^{n_q}$ and measurement noise $r_k \in \mathbb{R}^{n_r}$ are mutually independent with covariance matrices $Q_{k-1} \in \mathbb{R}^{n_q \times n_q}$ and $R_k \in \mathbb{R}^{n_r \times n_r}$, respectively. The state estimation problem aims at providing approximations for the mean $\hat{x}_k = \mathrm{E}[x_k]$ and covariance $P_k^{xx} = \mathrm{E}[(x_k \ominus \hat{x}_k)\,(x_k \ominus \hat{x}_k)^T]$ that characterize the *a posteriori* probability density function (PDF) $\rho(x_k|y_{1:k})$.

Due to the nonlinear characteristics of the model, our proposition is to use as basis to our approach the unscented Kalman filter (UKF) [29]. In the standard form of the UKF two problems arise when it is used to estimate attitude: (i) the UKF pertains to Euclidean systematization, therefore containing sum and weighting operations, which are not defined for unit quaternions; (ii) the output measured noise r_k can have time-varying statistical properties, which can, in the worst case, lead to diverging estimates. Regarding (i), most of the issues are solved if the modified unscented transform presented in Section III-D is applied in the place of the standard one, as shown in Section V-A. The solution of (ii) is our core contribution. We consider two events that may change the statistical properties of measured noise: a dynamic event, such as linear accelerations that mask the gravity vector projection measured by accelerometers; and a external influence, such as a ferromagnetic element that disturbs the Earth's magnetic field measured by the magnetometers. The rejection of these perturbations are addressed in sections V-B and V-C.

A. Quaternion-based UKF

The UKF algorithm presented in this section is based on the ones shown in [8], [14], which are slightly modified to encompass direct unit quaternion measurements and multiplicative noise in the process. Henceforth, the notation $\hat{x}_{k|k-1}$ indicates an estimate of x_k at time k based on information available up to and including time $k-1$. Likewise, $\hat{x}_k$ indicates an estimate of x_k at time k based on information available up to and including time k. Let the process noise be partitioned as $q_{k-1} \triangleq \begin{bmatrix} q_{1,k-1}^T & q_{2,k-1}^T \end{bmatrix}^T \in \mathbb{R}^{n_q}$ with covariance matrix $Q_{k-1} \triangleq \mathrm{diag}\left(Q_{1,k-1},\, Q_{2,k-1}\right) \in \mathbb{R}^{n_q \times n_q}$, where $q_{1,k-1} \in \mathbb{R}^{n_q - n_x + 1}$ is the noise nonlinearly related to the state vector and $q_{2,k-1} \in \mathbb{R}^{n_x - 1}$ is the linear partition of noise. To improve the numerical stability of the filter, additive noise is considered for all states [30].

Given these definitions, the modified UKF *forecast* step is given by

$$\left(\hat{x}_{k|k-1}, \tilde{P}_{k|k-1}^{xx}, \emptyset\right) = \mathrm{UT}\left(\hat{\breve{x}}_{k-1}, P_{k-1}^{\breve{x}\breve{x}}, u_{k-1}, f\right), \tag{23}$$

$$P_{k|k-1}^{xx} = \tilde{P}_{k|k-1}^{xx} + Q_{2,k-1}, \tag{24}$$

$$\left(\hat{y}_{k|k-1}, \tilde{P}_{k|k-1}^{yy}, P_{k|k-1}^{xy}\right) = \mathrm{UT}\left(\hat{x}_{k|k-1}, P_{k|k-1}^{xx}, 0, h\right), \tag{25}$$

$$P_{k|k-1}^{yy} = \tilde{P}_{k|k-1}^{yy} + R_k, \tag{26}$$

$$\nu_k = y_k \ominus \hat{y}_{k|k-1}, \tag{27}$$

where ν_k is the innovation. The augmented state vector $\breve{x}_{k-1} \in \mathbb{R}^{\breve{n}}$ and the corresponding covariance matrix $P_{k-1}^{\breve{x}\breve{x}} \in \mathbb{R}^{\breve{n}\times\breve{n}}$ are respectively given by

$$\breve{x}_{k-1} \triangleq \left[\, x_{k-1}^T\ q_{1,k-1}^T \,\right]^T,$$

$$P_{k-1}^{\breve{x}\breve{x}} \triangleq \begin{bmatrix} P_{k-1}^{xx} & [0]_{(n_x-1)\times(n_q-n_x+1)} \\ [0]_{(n_q-n_x+1)\times(n_x-1)} & Q_{1,k-1} \end{bmatrix},$$

with $\breve{n} = n_q + 1$.

The state estimate and error covariance matrix are updated using information from y_k in the *data-assimilation* step, given by:

$$K_k = P^{xy}_{k|k-1}\left(P^{yy}_{k|k-1}\right)^{-1}, \tag{28}$$

$$\hat{x}_k = \hat{x}_{k|k-1} \oplus K\nu_k, \tag{29}$$

$$P^{xx}_k = P^{xx}_{k|k-1} - K_k P^{yy}_{k|k-1} K_k^T. \tag{30}$$

B. Adaptive Covariance Matrix

The uncertainty of measurements in the UKF is represented by covariance matrix R_k, which is usually constant. However, the measurement uncertainties can be time-varying. We then propose the use of innovation ν_k to adjust the measurement covariance matrix online through the covariance matching (CM) approach [15].

Based on the assumption that the observation covariance matrix R_k is constant during a sliding sampling window with finite length N, the basic idea of CM is to make the innovation ν_k consistent with its covariance $E[\nu_k\nu_k^T] \triangleq P^{yy}_{k|k-1}$. Notice that, the innovation pertains to the 3-dimensional Euclidean *tangent space*. Thus, the covariance of ν_k is estimated as based on the last N innovation samples as

$$E[\nu_k\nu_k^T] \approx \frac{1}{N}\sum_{j=k-N+1}^{k} \nu_j\nu_j^T. \tag{31}$$

Notice that, the UKF (see Equation (26)) approximates the covariance by $E[\nu_k\nu_k^T] \triangleq \tilde{P}^{yy}_{k|k-1} + R_k$, where $\tilde{P}^{yy}_{k|k-1} \triangleq \sum_{j=1}^{2(n-1)} w_j \tilde{y}_{j,k|k-1}\tilde{y}^T_{j,k|k-1}$. Then, R_k can be estimated by

$$\hat{R}_k = \frac{1}{N}\sum_{j=k-N+1}^{k} \nu_j\nu_j^T - \tilde{P}^{yy}_{k|k-1}. \tag{32}$$

To avoid negative values due the subtraction operation in (32), negative values in $\hat{R}_k$ are replaced by its correspondent value in the nominal covariance matrix R_0.

C. Outlier Rejection

Outliers are spurious data that contaminate the statistical distribution. The contaminated measurements deviate significantly from the normal observations, which directly reflects in the innovation value ν_k, and, consequently, in the covariance estimated by CM.

The Hampel identifier [26] is an outlier identification method that is reported as extremely effective in practice [31]. Based on this approach, our contribution is to compute a gain $\lambda \in \mathbb{R}^{n_r \times n_r}$ to be used as a multiplier that reduces the outlier influence in the estimation of the covariance matrix and also on the Kalman gain. This gain is a diagonal matrix, wherein each the diagonal is defined as

$$\lambda_{j,ii} \triangleq \min\left(1,\ \frac{n_\sigma s_i}{|\nu_{j,i} - \mathrm{med}\{\nu_{j,i}\}|}\right), \tag{33}$$

where $s_i = 1.4826\,\mathrm{med}\{|\nu_{j,i} - \mathrm{med}\{\nu_{j,i}\}|\}$ is the median absolute deviation (MAD), n_σ is the number of standard deviations (confidence region) by which the innovation sample must differ from the local median, med is the median operator, $\{\cdot\}$ is a moving window with size N, $j \triangleq k-N+1 \ldots k$ is an index for each element of the moving window, and i is the index of each element of the innovation vector.

D. Robust Adaptive Unscented Kalman Filter

By combining (32) and (33) with the UKF Equations (23)-(30), we then obtain a three step algorithm that we call Robust Adaptive Unscented Kalman Filter (RAUKF). The first step is the *forecast* step, which is given by (23)-(25) and (27). The second step, is the *robust noise estimation* given by (33), the estimate covariance

$$\hat{R}_k = \max\left(\frac{1}{N}\sum_{j=k-N+1}^{k} \lambda_j\nu_j\left(\lambda_j\nu_j\right)^T - \tilde{P}^{yy}_{k|k-1}, R_0\right) \tag{34}$$

and (26). The third and last step is the *data-assimilation* step, which is given by (28), (30), and

$$\hat{x}_k = \hat{x}_{k|k-1} \oplus K\lambda_k\nu_k\,. \tag{35}$$

VI. Experimental Results and Discussion

In this section we compare the performance of the proposed RAUKF algorithm with the classical UKF algorithm for quaternions, the complementary filter (CF) proposed in [9], and the commercial algorithm embedded in the MicroStrain 3DM-GX1® IMU. We implemented RAUKF using Matlab. Our code is available at `https://bitbucket.org/coroufmg/raukf_cm`. Four disturbance scenarios were evaluated: (i) abrupt and (ii) slow varying magnetic disturbances; (iii) linear accelerations; and iv) rotation about the origin. Actual data was collected at 40Hz from the IMU, which was mounted on the end effector of a Comau Smart Six manipulator, used to perform controlled movements and to provide accurate orientation information.

To set UKF and RAUKF, we have assumed that the covariance matrix $Q_{1,k-1} \in \mathbb{R}^{3\times3}$ is diagonal with elements related to the angular rates measured by the gyros. This matrix was estimated as $\sigma_\omega = [0.008\ 0.0065\ 0.0086]^T$rad/s from a temporal window in a steady-state behavior. The additive noise of process was represented by the diagonal matrix $Q_{2,k-1} \in \mathbb{R}^{6\times6}$. This matrix is related to the attitude, parametrized as a rotation vector, and the bias terms of the gyros. The standard deviations were empirically set as $\sigma_\mathrm{v} = \left[1\times10^{-20}\right]_{3\times1}$rad and $\sigma_\beta = \left[1\times10^{-9}\right]_{3\times1}$rad/s, for attitude and bias terms, respectively. The covariance matrix of measurements R_k is computed by the UT. The measured acceleration and magnetic field are propagated through the nonlinear function represented by equations (20)-(22). Standard deviations of accelerometer and magnetometer are $\sigma_\mathrm{a} = [0.0361\ 0.0455\ 0.0330]^T$m/s^2 and $\sigma_\mathrm{m} = [0.0011\ 0.00098\ 0.00098]^T$Gauss [G], respectively, which were estimated from a temporal window of collected data with a steady-state behavior. The sliding window size of RAUKF was empirically set to be $N = 20$ samples, which represents a period of 0.5 s during which the noise covariance is assumed to be constant, and the confidence region $n_\sigma = 3$ standard deviations. CF has two parameters, the gain that quantifies the gyro measurement noise, set as $\beta = 0.007$,

TABLE I

ROOT MEAN SQUARE ERROR (RMSE) IN DEGREES. THE LOWEST RMSE RESULTS ARE HIGHLIGHTED IN BOLD.

	Abrupt Magn.			Slow Magn.			Linear acc.			Rotat. around the orig.		
Algorithm	$\tilde{\phi}$	$\tilde{\theta}$	$\tilde{\psi}$	$\tilde{\phi}$	$\tilde{\theta}$	$\tilde{\psi}$	$\tilde{\phi}$	$\tilde{\theta}$	$\tilde{\psi}$	$\tilde{\phi}$	$\tilde{\theta}$	$\tilde{\psi}$
RAUKF	0.30	0.90	**0.48**	**0.07**	**0.09**	**1.84**	**0.28**	**0.87**	**0.16**	**1.08**	**1.31**	**0.91**
UKF	0.30	0.90	0.62	0.98	0.51	13.0	4.0	3.78	2.36	1.97	1.73	2.23
CF	0.30	0.90	0.60	9.22	11.00	28.90	1.87	1.60	0.53	1.17	1.61	1.17
3DM-GX1	0.34	1.00	0.54	0.12	**0.09**	11.28	0.37	0.99	0.39	**1.08**	1.34	1.37

and the gain that quantifies the bias terms, set as $\zeta = 0.01$. These values follows the authors recommendations [9].

A. Magnetic Field Distortion

In our first experiment, the magnetic brakes of the robot manipulator are turned on and off a few times, thus causing an abrupt variation in the magnetic field that is perceived by the magnetometers. Figure 1a shows the linear acceleration, and the magnetic field, in the y-axis direction. Observe that jumps in the magnetic field were generated. Due to the shaking caused by the release of the brakes, some spikes of acceleration also appear. Videos of this and other experiments are found this link: `https://goo.gl/mtFSqG`. Figure 1b shows the heading error for each algorithm. Notice that, UKF and CF algorithms are more sensitive to the perturbations, converging quickly to measurements even with abnormal behavior.In contrast, RAUKF and 3DM-GX1 estimates converge slowly to measurements in the presence of abnormal behavior. However, RAUKF is less sensitive to short duration perturbations and converges faster to the measurement as the disturbance is over.

In a second experiment, the magnetic field was artificially and slowly disturbed with a magnetic material. This kind of perturbation is usually difficult to detect and can damage the estimation. Notice that, RAUKF is the less sensitive to the slow varying abnormal measurement. CF yields the worst results as shown by Root Mean Square Error (RMSE) in Table I. The abnormal behavior of magnetic field affects the bias estimates of angular rate in the z-direction for UKF and in all directions for CF-M (not shown).

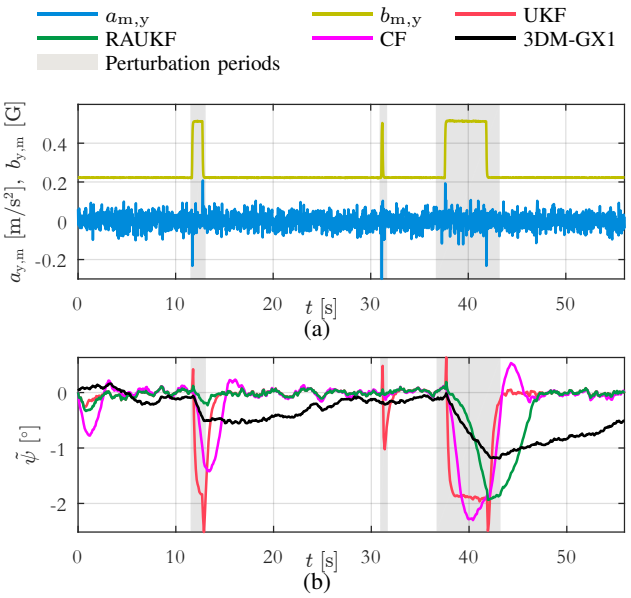

Fig. 1. (a) Linear acceleration a_m and magnetic field b_m measurements in the y-axis direction and (b) the error $\tilde{\psi}$ of heading angle.

B. Linear Acceleration Disturbance

To test the behavior of the algorithms against the perturbation of linear velocities, the manipulator executed independent translational movements in each axis. We observed that, even the movements being executed separately in each axis, linear accelerations appear in all axis. This is probably due to a small angle in the link joining the IMU and the robot end effector. Table I shows the values of RMS for this and other experiments. Notice that, the UKF provides the worst results. In contrast, RAUKF yields the best RMSE indexes and the smallest peak-error.

C. Rotations Around the Origin

In our last experiment presented in this paper, rotations around the origin in each axis were performed. In this case, estimates are influenced by linear accelerations that appear due to a lever arm between the IMU and the robot end effector. Again, the proposed algorithm yields the best results as shown in Table I.

VII. CONCLUSIONS

In this work, a robust adaptive unscented Kalman filter for orientation estimation using quaternions was presented. The algorithm ensures the unit norm of quaternion in all algorithm steps without forcing a normalization. The exponential map of quaternions is used to parametrize the error quaternion. This parameterization allows us to perform operations in Euclidean space and then use existing approaches to adapt the measurement covariance matrix and detect outliers.

The proposed algorithm was compared to a nonadaptive version of UKF, a complementary filter, and commercial algorithm embedded in the IMU. Some experiments were performed to verify the performance of the algorithms in situations were distorted magnetic field and linear accelerations exist. The proposed algorithm shows the best RMSE results in all situations tested, and the smallest peak-error for linear acceleration disturbance.

REFERENCES

[1] P. Vartiainen, T. Bragge, J. P. Arokoski, and P. A. Karjalainen, "Nonlinear State-Space Modeling of Human Motion Using 2-D Marker Observations," *IEEE Transactions on Biomedical Engineering*, vol. 61, no. 7, pp. 2167–2178, July 2014.

[2] T. Michel, P. Genevs, H. Fourati, and N. Layada, "On attitude estimation with smartphones," in *IEEE Intl. Conference on Pervasive Computing and Communications*, March 2017, pp. 267–275.

[3] H. Gui and A. H. de Ruiter, "Quaternion Invariant Extended Kalman Filtering for Spacecraft Attitude Estimation," *Journal of Guidance, Control, and Dynamics*, vol. 41, no. 4, pp. 863–878, 2017.

[4] G. A. S. Pereira, P. Iscold, and L. A. B. Torres, "Airplane attitude estimation using computer vision: simple method and actual experiments," *Electronics Letters*, vol. 44, no. 22, pp. 1303–1304, 2008.

[5] R. Costanzi, F. Fanelli, N. Monni, A. Ridolfi, and B. Allotta, "An Attitude Estimation Algorithm for Mobile Robots Under Unknown Magnetic Disturbances," *IEEE/ASME Transactions on Mechatronics*, vol. 21, no. 4, pp. 1900–1911, Aug 2016.

[6] J. S. Jang and D. Liccardo, "Small UAV automation using MEMS," *IEEE Aerospace and Electronic Systems Magazine*, vol. 22, no. 5, pp. 30–34, 2007.

[7] P. D. Groves, *Principles of GNSS, inertial, and multisensor integrated navigation systems*. Artech house, 2013.

[8] B. J. Sipos, "Application of the manifold-constrained unscented Kalman filter," in *2008 IEEE/ION Position, Location and Navigation Symposium*, May 2008, pp. 30–43.

[9] S. O. Madgwick, "An efficient orientation filter for inertial and inertial/magnetic sensor arrays," University of Bristol (UK), Tech. Rep., 04 2010.

[10] R. G. Valenti, I. Dryanovski, and J. Xiao, "A linear Kalman filter for MARG orientation estimation using the algebraic quaternion algorithm," *IEEE Transactions on Instrumentation and Measurement*, vol. 65, no. 2, pp. 467–481, 2016.

[11] E. J. Lefferts, F. L. Markley, and M. D. Shuster, "Kalman filtering for spacecraft attitude estimation," *Journal of Guidance, Control, and Dynamics*, vol. 5, no. 5, pp. 417–429, 1982.

[12] J. L. Crassidis and F. L. Markley, "Unscented filtering for spacecraft attitude estimation," *Journal of Guidance Control and Dynamics*, vol. 26, no. 4, pp. 536–542, 2003.

[13] C. Hertzberg, R. Wagner, U. Frese, and L. Schröder, "Integrating generic sensor fusion algorithms with sound state representations through encapsulation of manifolds," *Information Fusion*, vol. 14, no. 1, pp. 57–77, 2013.

[14] H. T. Menegaz and J. Y. Ishihara, "Unscented and square-root unscented Kalman filters for quaternionic systems," *International Journal of Robust and Nonlinear Control*, pp. 1–28, 2018.

[15] R. Mehra, "Approaches to adaptive filtering," *IEEE Transactions on Automatic Control*, vol. 17, no. 5, pp. 693–698, Oct 1972.

[16] X. R. Li and Y. Bar-Shalom, "A recursive multiple model approach to noise identification," *IEEE Transactions on Aerospace and Electronic Systems*, vol. 30, no. 3, pp. 671–684, Jul 1994.

[17] C. Hide, T. Moore, and M. Smith, "Adaptive Kalman filtering algorithms for integrating GPS and low cost INS," in *Position Location and Navigation Symposium*, 2004, pp. 227–233.

[18] A. Moghaddamjoo and R. L. Kirlin, "Robust adaptive Kalman filtering with unknown inputs," *IEEE Transactions on Acoustics, Speech, and Signal Processing*, vol. 37, no. 8, pp. 1166–1175, Aug 1989.

[19] R. K. Pearson, Y. Neuvo, J. Astola, and M. Gabbouj, "Generalized Hampel Filters," *EURASIP Journal on Advances in Signal Processing*, vol. 2016, no. 1, p. 87, Aug 2016.

[20] H. E. Soken and C. Hajiyev, "Pico satellite attitude estimation via robust unscented Kalman filter in the presence of measurement faults," *ISA transactions*, vol. 49, no. 3, pp. 249–256, 2010.

[21] D. Lee, G. Vukovich, and R. Lee, "Robust Adaptive Unscented Kalman Filter for Spacecraft Attitude Estimation Using Quaternion Measurements," *Journal of Aerospace Engineering*, vol. 30, no. 4, p. 04017009, 2017.

[22] M. Ghobadi, P. Singla, and E. T. Esfahani, "Robust Attitude Estimation from Uncertain Observations of Inertial Sensors Using Covariance Inflated Multiplicative Extended Kalman Filter," *IEEE Transactions on Instrumentation and Measurement*, vol. 67, no. 1, pp. 209–217, 2018.

[23] M. Euston, P. Coote, R. Mahony, J. Kim, and T. Hamel, "A complementary filter for attitude estimation of a fixed-wing UAV," in *2008 IEEE/RSJ International Conference on Intelligent Robots and Systems*, Sept 2008, pp. 340–345.

[24] S. O. H. Madgwick, A. J. L. Harrison, and R. Vaidyanathan, "Estimation of IMU and MARG orientation using a gradient descent algorithm," in *IEEE Intl. Conf. on Rehabilitation Robotics*, June 2011, pp. 1–7.

[25] R. G. Valenti, I. Dryanovski, and J. Xiao, "Keeping a good attitude: A quaternion-based orientation filter for IMUs and MARGs," *Sensors*, vol. 15, no. 8, pp. 19 302–19 330, 2015.

[26] L. Davies and U. Gather, "The identification of multiple outliers," *Journal of the American Statistical Association*, vol. 88, no. 423, pp. 782–792, 1993.

[27] S. Kim, R. Haschke, and H. Ritter, "Gaussian mixture model for 3-Dof orientations," *Robotics and Autonomous Systems*, vol. 87, pp. 28–37, 2017.

[28] A. C. B. Chiella, B. O. S. Teixeira, and G. A. S. Pereira, "Adaptive Estimators for Localization of Acrobatic Airplanes Equipped with Cameras (under review)," 2019.

[29] S. J. Julier and J. K. Uhlmann, "Unscented filtering and nonlinear estimation," *Proceedings of the IEEE*, vol. 92, no. 3, pp. 401–422, 2004.

[30] K. Xiong, H. Zhang, and C. Chan, "Performance evaluation of UKF-based nonlinear filtering," *Automatica*, vol. 42, no. 2, pp. 261–270, 2006.

[31] R. K. Pearson, "Outliers in process modeling and identification," *IEEE Transactions on Control Systems Technology*, vol. 10, no. 1, pp. 55–63, Jan. 2002.